Delft University of Technology
Faculty Of Civil Engineering

ADDITIONAL THESIS REPORT

Study on synergies in the removal of organic micropollutants using combined iron electrocoagulation and irradiation

Supervisors:

Prof. Dr. Ir. Doris van Halem

Ir. Mrinal Roy

Submitted by:

Akhilesh Soodan

MSc Civil Engineering (track Environmental Engineering)

Student Number- 5594758

Table of Contents

List of Tables

List of Figures

Title

Study on synergies in the removal of organic micropollutants during combined iron electrocoagulation and irradiation by a solar simulator.

Abstract

This study analyses the removal of organic micropollutants (OMPs) through iron electrocoagulation in the presence of solar radiation. Methylene Blue (MB) dye has been considered as a contaminant which is removed by the action of highly reactive oxygen species (ROS) formed as intermediates during electrocoagulation (charge dosage, CD = 30 C/L and charge dosage rate, CDR = 5 C/L/min). The impact of pH on the removal rate is observed throughout the experiment. The effect of radiation (300-400 nm, 65 W/m2) on electrocoagulation has been further studied by performing iron electrocoagulation in a solar simulator (ECS) and comparing it with iron electrocoagulation in the air (EC), iron electrocoagulation with H_2O_2 – electro-fenton process (EF) and iron electrocoagulation with H_2O_2 in a solar simulator– photo-electro-fenton process in a solar simulator (PEF). The results of MB removal efficiency for each process can be deduced as: PEF = EF > ECS > EC; which conveys that combined electrocoagulation and solar radiation has synergies in the removal of OMPs, while there's no impact of solar radiation in case of PEF when compared to EF. Further, the concentration removal capability in PEF and EF decline with the pH increasing from 3 to 9, while in case of EC and ECS, there's is a slight improvement in the concentration removal from pH 6 to pH 8.

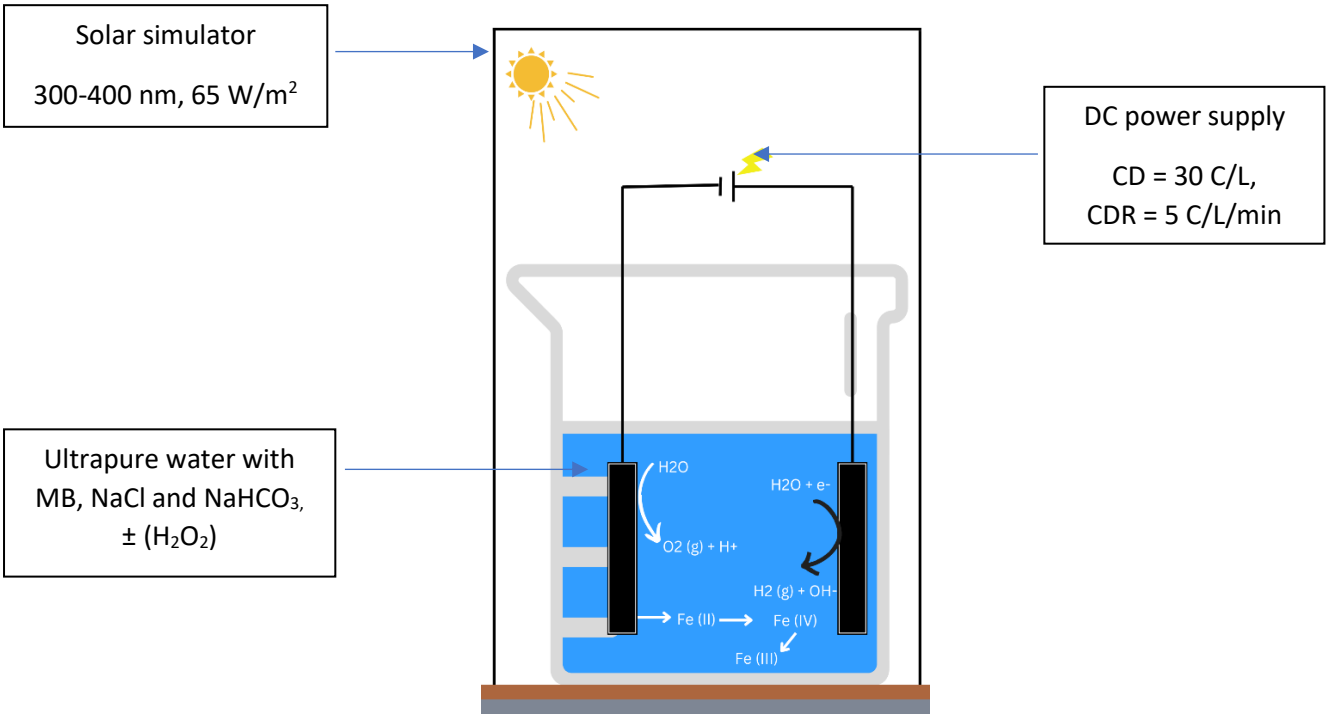

Figure 1: Combined electrocoagulation and radiation experiment

Keywords: electrocoagulation, fenton, solar radiation, organic micropollutants, methylene blue, photo electrocoagulation, charge dosage, ROS

Highlights

- Exposure to solar radiation has a significant impact on MB removal in the case of EC and ECS while the impact is not pronounced in EF and PEF.
- Wavelength of the radiation is an important factor in the generation of ROS.
- The degree of contribution in the removal of OMPs – ROS or adsorption has dependence on the pH of the system

1. Introduction

Organic micropollutants pose major environmental and health risks (**Gaspar F.W. et. al. 2014**) (**Rosal et. al., 2010**). The European Union has been consistently updating the watchlist of harmful chemicals which are found in day-to-day products and seep into surface waters (**European Commission, 2020**). These chemicals are difficult to remove by conventional water treatment processes and need to be treated through methods such as advanced oxidation (**Deng et. al., 2015**) (**Rosal et. al., 2010**). Fenton process has been widely used as an advanced oxidation process in which Fe2+ reacts with H_2O_2 to produce strong ROS- $^{\cdot}OH$ for the removal of impurities (**Deng et. al., 2015**). It has been observed that the photo-fenton process can occur naturally in the environment in the case of sunlit fresh waters in which both H_2O_2 and Fe(II) are photochemically produced (**Southworth et. al., 2003**). Solar radiation has also been proven to remove arsenic from groundwater in Bangladesh with the help of already-present iron and few drops of lemon juice in ultraviolet-C transparent polyethylene bottles (**Wegelin, et. al., 2000**). This means that exposure to sunlight can facilitate the formation of ROS, through the photo-fenton process, which can remove pollutants from water.
In EC, coagulant species get dissolved from metal electrodes, forming metal ions as coagulants which in-turn form hydroxides by combining with the OH- ions. Iron has been widely used for EC owing to its availability and high valence which is advantageous through good coagulation efficiency (**Gregory J., 2005**). The anodic dissolution of Fe(0) leads to the formation of Fe (II). Fe (II) oxidation results in Fe (III) formation, which polymerizes and creates high-adsorbing Fe (III) precipitates (**Genuchten et. al., 2014**) (**Lakshmanan et. al., 2009**). This high adsorption affinity can be utilized efficiently for the treatment of drinking water by binding heavy metals such as arsenic, pathogens and other impurities such as OMPs (**D. Ghernaout, 2019**) (**Bandaru et. al. 2020**) (**Bicudo et. al., 2020**). Also, during iron EC, there's a production of reactive oxygen species (ROS) such as $^{\cdot}OH$ and $^{\cdot}O_2^-$ and high valence iron species such as Fe (IV) through intermediate reactions, and these can potentially oxidize the impurities (**Li, et al., 2012**) (**D. Ghernaout, 2013**). Therefore, both adsorption by Fe (III) precipitates and generation of ROS intermediates can be effective mechanisms to target OMPs. The contribution of oxidant compounds originating from EC has been previously analysed for the removal of estrogenic compounds in water and shown that 0 – 12% removal of these compounds in the experiment was due to Fe (IV) species (**Maher et. al., 2019**). Electrocoagulation has been experimented in effluent treatment for paper and pulp industry (**Jaafarzadeh et. al., 2016**) as well as distillery (**P. Asaithambi et. al. 2016**) with sulphate radicals and ·OH radicals in focus respectively. The removal of OMPs through a combination of EC and solar radiation has been performed in previous studies (**Maher et. al, 2019**) (**Brillas E., 2020**) (**Farhadi S et. al, 2012**). There are multiple mechanisms that control Fe (II) production as well as oxidation, with pH being one of the important factors (**Longqian Xu, et. al., 2017**). pH has a direct impact on the metal dissolution and type of chemical formation, coagulation efficiency and floc formation (**Weiss et. al. 2021**), and the type of ROS formed (**Hug S. J. et. al. 2003**) (**Yufan Chen et. al., 2022**).
However, the existing literature is not able to provide information on how the synergies between electrocoagulation and solar radiation work over a wide pH range. It also provides limited clarification on the underlying factors which result in the different OMP removal efficiencies for the processes such as EC, ECS, EF and PEF. This study is performed for experiments EC, ECS, EF and PEF over a pH range from 3-9 and their OMP removal

efficiency has been analyzed. Dye methylene blue (MB) has been considered a contaminant and its removal by utilizing the abovementioned processes at different pH has been performed for comparative studies.

Commonly used abbreviations

EC: Electrocoagulation in the presence of air

ECS: EC in a solar simulator

EF: Electro-fenton process

PEF: Photoelectro-fenton process

CD: Charge dosage

CDR: Charge dosage rate

MB: Methylene Blue

ROS: Reactive Oxygen Species

Fundamentals of electrocoagulation

Reactions in the system (**Li L. et. al., 2012**) (**Shiwei et. al., 2022**):

Anode: $Fe\ (0) \longrightarrow Fe\ (II) + 2e^-$ **(1)**

Cathode: $2H_2O + 2e^- \longrightarrow H_2\ (g) + 2OH^-$ **(2)**

Intermediate reactions:

$Fe\ (II) + O_2 \longrightarrow \cdot O_2^- + Fe\ (III)$ **(3)**

$Fe\ (II) + \cdot O_2^- + 2H^+ \longrightarrow Fe\ (III) + H_2O_2$ **(4)**

$Fe\ (II) + H_2O_2 \longrightarrow Fe\ (III) + \cdot OH + OH^-$ **(5)**

$Fe\ (II) + H_2O_2 \longrightarrow Fe\ (IV) + O + H_2O$ **(6)**

$3Fe\ (II) + O_2 \longrightarrow Fe\ (IV) + 2Fe\ (III)$ **(7)**

$Fe\ (IV) + Fe\ (II) \longrightarrow Fe\ (III)$ **(8)**

Weight of Fe(II) dosed

The charge dosage (CD) is an important factor in determining the coagulant production (**Kobya M. et. al., 2016**) (**Amrose S. et. al., 2013**). It helps in calculating the weight of dissolved Fe anode, which is given by the Faraday's Law:

$W = qM / nF$ **(9)**

$dq/dt = i / V$ **(10)**

where W is weight of Fe anode dosed in mg/L, q is CD in C/L, M is molecular weight of Fe = 55.845 mg/L, n is number of transferred electrons i.e. 2 in case of Fe, F is Fraday's constant = 96,485 C/mol, charge dosage rate (CDR) is dq/dt in C/L/min, i is current in mA and V is the volume of the electrocoagulation cell.

2. Hypothesis

Ho: Iron electrocoagulation and solar simulation do not have a synergistic effect in the removal of MB.

Ha: Iron electrocoagulation and solar simulation have a synergistic effect in the removal of MB.

Assuming Ho is incorrect, the below graph between the percentage MB removal and pH for each of EC, ECS, EF and PEF is predicted.

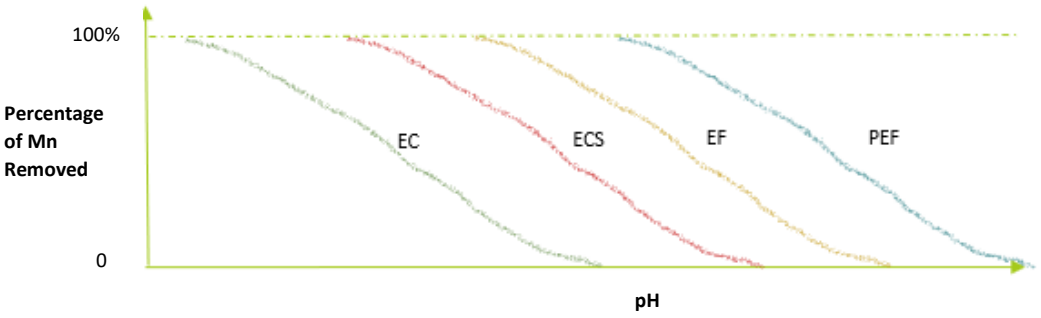

Figure 2: Hypothesised behaviour of EC, ECS, EF and PEF experiments

2.1 Objectives:

- Study removal of the probe compound (MB) by EC, ECS, PE and PEF individually
- Observe synergies during ECS and PEF in removal of MB
- Deduce mechanisms behind MB removal at different pH for EC, ECS, PE and PEF

3. Materials and Methods

3.1 Experimental Setup:

The set up for an electrocoagulation cell (Fig 2.a) consisted of a 1 litre cylindrical glass beaker placed on a magnetic stirrer. A pair of 1mm thick iron plates with an approximate interelectrode distance of 6mm were inserted in the beaker with the help of a vertical mount. These plates were in-turn connected to a DC current supplier (TENMA R 72–10,500) for which the current setting was kept constant at 0.065A. The setup was placed on a small table open to the atmosphere.

In order to simulate solar radiation, a solar simulator Atlas Suntest XXL+ was used. The solar simulator was calibrated to give radiation in the range 300-400 nm and an irradiance of 65 W/m^2. The experiments involving solar simulation had a variation (Fig 2.a) in the plate holding mount and the steel plates used (interelectrode distance approx. 6mm). The change was made owing to lack of space in the solar simulator and hence a different set up was needed in this case. However, the charge dosage and charge dosage rate were kept same as in the

case without solar simulation, which implies that the iron dissolved into the solution from anode remains constant.

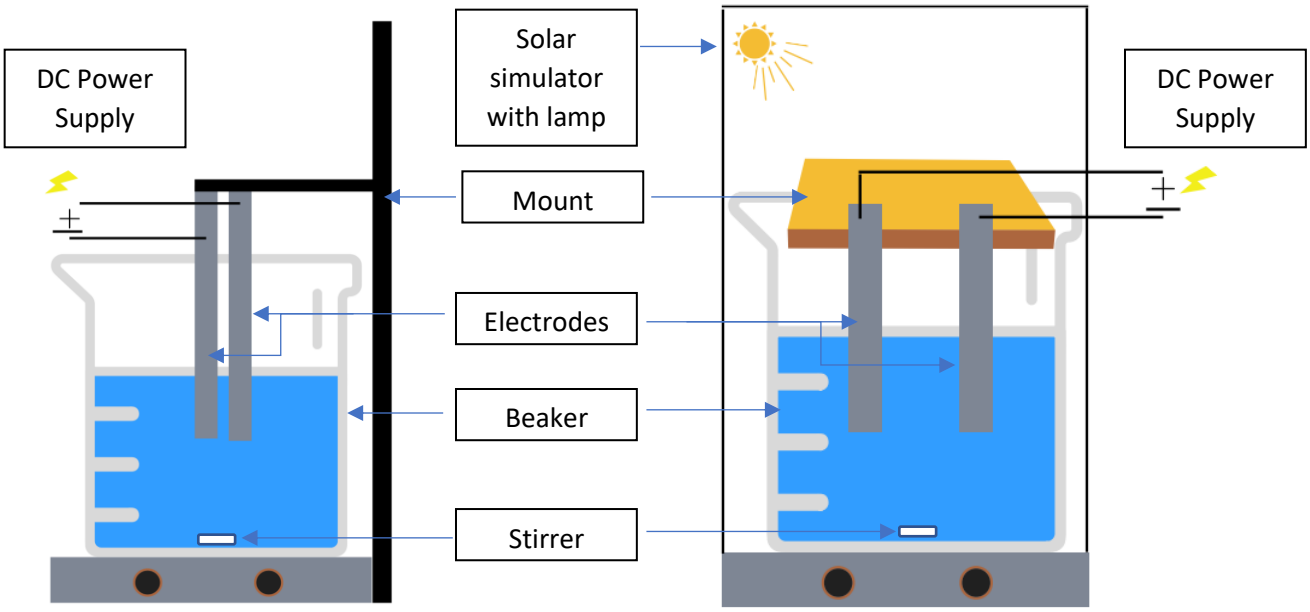

Figure 3.a: Apparatus for EC and ECS

Figure 3.b: Apparatus for EF and PEF

3.2 Chemicals

- 0.05 mg of dry MB powder (IUPAC name: 7-(dimethylamino)phenothiazin-3-ylidene, formula: C16H18ClN3S**)** added to 500 mL of ultrapure water making 5 mg/L stock
- NaCl as a supporting electrolyte (3.5 mg / 800 mL water)
- $NaHCO_3$ as a pH buffer (0.3 mg / 800 mL water)
- 0.1 mL of 333 g/L of H_2O_2 added to 9.9 mL ultrapure water to prepare a stock solution of 3.33 g/L
- 1M HCl and 1M NaOH for pH modification

3.3 Analytical Equipment

The concentration changes were measured by first measuring absorbance using a UV-Vis spectrophotometer: Genesys 10S UV Vis. The absorbance values measured can then be converted to concentrations by developing a MB calibration curve.

MB calibration followed a linear relation from 0 - 12 mg/L which can be written as:

Concentration MB = 4.952 * (Absorbance) - 0.4891 **(11)**

The absorbance values are measured at 664 nm since peak in the absorption spectrum of MB occurs at around 664 nm (**Amparo, 2019**).

3.4 Statistical Analysis

Statistical analysis was done on the experimental data with the help of one-way ANOVA and t-test. However, it needs to be noted that both these tests assume the data to be in a normal distribution and homogeneity of variances in the entries between the groups (**CCNMLT, 2022**). The same assumption was taken for the readings obtained in the experiment. One-way ANOVA was performed on the final concentration readings (post-experiment) obtained across the pH 5 - 9 for EC, ECS, PEF and EF. t-tests were performed between the final concentration values of EC and ECS and, between EF and PEF. Both test help in providing information on whether there is a significant difference between the mean values of different groups. t-test was used instead of ANOVA to avoid false positive errors.

3.5 Research Design

The following design is created to carry out the research:

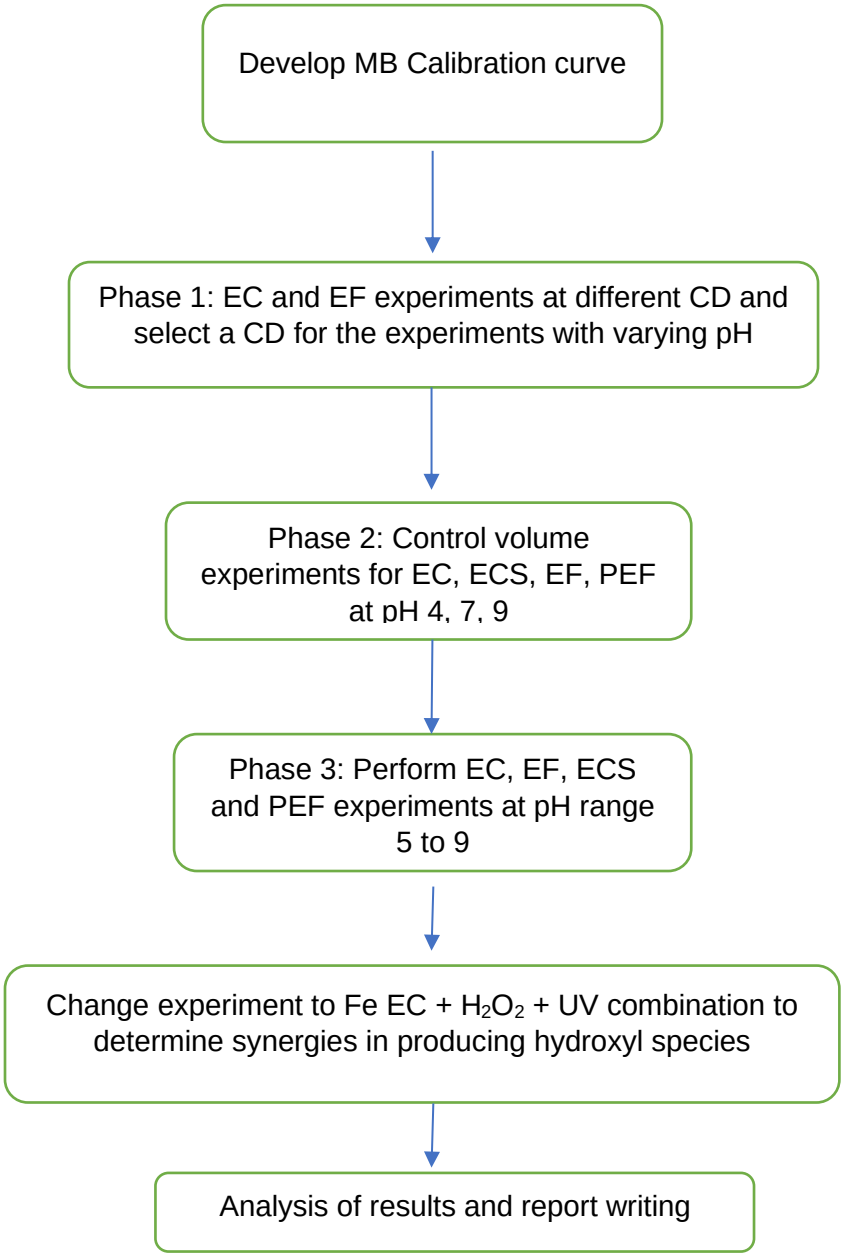

Figure 4: Flow chart of the experiment

3.6 Experiment

Before starting any experiment, few standard procedures were done:

- The glassware was washed in soap and water and rinsed with demineralised (demi) water
- Before and after each experiment, electrodes were polished with a sandpaper to remove the build-up of scale and washed with demi water
- MB stock in ultrapure water was prepared at the start of every day of experimentation
- In case of experiments involving H_2O_2, H_2O_2 stock in ultrapure water was prepared. The molar ratio of H_2O_2 dosing to Fe (II) dissolved into the system was 1:1

Synthetic wastewater

The synthetic wastewater was created by adding 4 mL of the MB stock solution in 800 mL ultrapure water (using Millipore MilliQ 18.2 MΩ at 22±1 °C) along with 3.5 g of NaCl and 0.3 g $NaHCO_3$ (weighing done by analytical scale Mettler-Toledo 240). In case of experiments involving H_2O_2 dosing (EF and PEF), 1.43 mL of H_2O_2 stock is also added.

The experiments performed in the study can be categorised into three phases:

Phase 1: Electrocoagulation at different CDs

EC experiments were performed with CD at 30 C/L, 60 C/L, 120 C/L, 180 C/L, 240 C/L and 300 C/L. The CDR was kept constant at 5 C/L/min while the pH for all the tests was in the range 8.3 - 8.5. This resulted in the runtime of 6 min, 12 min, 24 min, 30 min, 45 min and 60 min for respectively. The setup is presented in figure 3.a.

EF experiments were performed with CD 10 C/L, 30 C/L and 60 C/L. The CDR was constant 5 C/L/min, pH = 3 and 1.43 mL of H2O2 was added. The runtime in this case was 2 min, 6 min and 10 min. The setup is presented in figure 3.a.

The corresponding increasing iron dosage in both the cases (EC and EF) can be found using equation 9.

In both the cases initial (time = 0) and final samples (time at the end of the experiment as per the defined CD) were taken using a syringe and a 20 µm filter. The absorbance values of the samples were measured and corresponding concentrations were found. It was observed that for EF at 30 CD, the MB removal reaches closer to zero. Given that phase 3 had multiple experiments involving H_2O_2, CD = 30 C/L was taken as an ideal choice for phase 3 and further.

Phase 2: Control volume experiments

Control volume experiments were performed at pH 4, 7 and 9 to set up a base-case criterion for the EC, ECS, EF and PEF experiments.

The experiments consisted of the following:

i) Synthetic water is stirred for 6 minutes

ii) Synthetic water with H_2O_2 is stirred for 6 minutes

iii) Synthetic water is kept in a solar simulator for 6 minutes, while stirring continuously

iv) Synthetic water with H_2O_2 is kept in a solar simulator for 6 minutes, while stirring continuously

In all the four cases initial (time = 0) and final samples (time = 6 min) were taken using a syringe and a 20 µm filter. The absorbance values of the samples were measured and corresponding concentrations were found.

Phase 3: EC, ECS, EF and PEF experiments at different pH

Iron dosing: A standard criteria for iron dosing in water through anodic dissolution during electrocoagulation was established for EC, ECS, PEF and EF experiments. This was done by fixing the CD to 30 C/L and CDR to 5 C/L/min. This gives total electrocoagulation time using equation 9 and equation 10 = CD / CDR = 6 min. Applying Faraday's Law in equation 9, Fe dosage = 8.68 mg/L = 156 µmol / L

In this phase, the following experiments were performed:

EC experiments consisted of running electrocoagulation in open air with CD 30 C/L and CDR 5 C/L/min for pH 5, 6, 6.5, 7, 7.5, 8, 9. The setup is presented in figure 3.a.

ECS experiments consisted of running electrocoagulation in a solar simulator with CD 30 C/L and CDR 5 C/L/min for pH 5, 6, 6.5, 7, 7.5, 8, 9. The setup is presented in figure 3.b.

EF experiments consisted of running electrocoagulation of H_2O_2 dosed synthetic water with CD 30 C/L and CDR 5 C/L/min for pH 3, 4, 5, 7, 7.5, 8, 9. The setup is presented in figure 3.a.

PEF experiments consisted of running electrocoagulation of H_2O_2 dosed synthetic water in a solar simulator with CD 30 C/L and CDR 5 C/L/min for pH 3, 4, 5, 7, 7.5, 8, 9. The setup is presented in figure 3.b.

All experiments involved constant stirring and pH modified with the help of adding few drops of 1M HCl or 1M NaOH.

4. Results

4.1 MB concentration removal vs pH

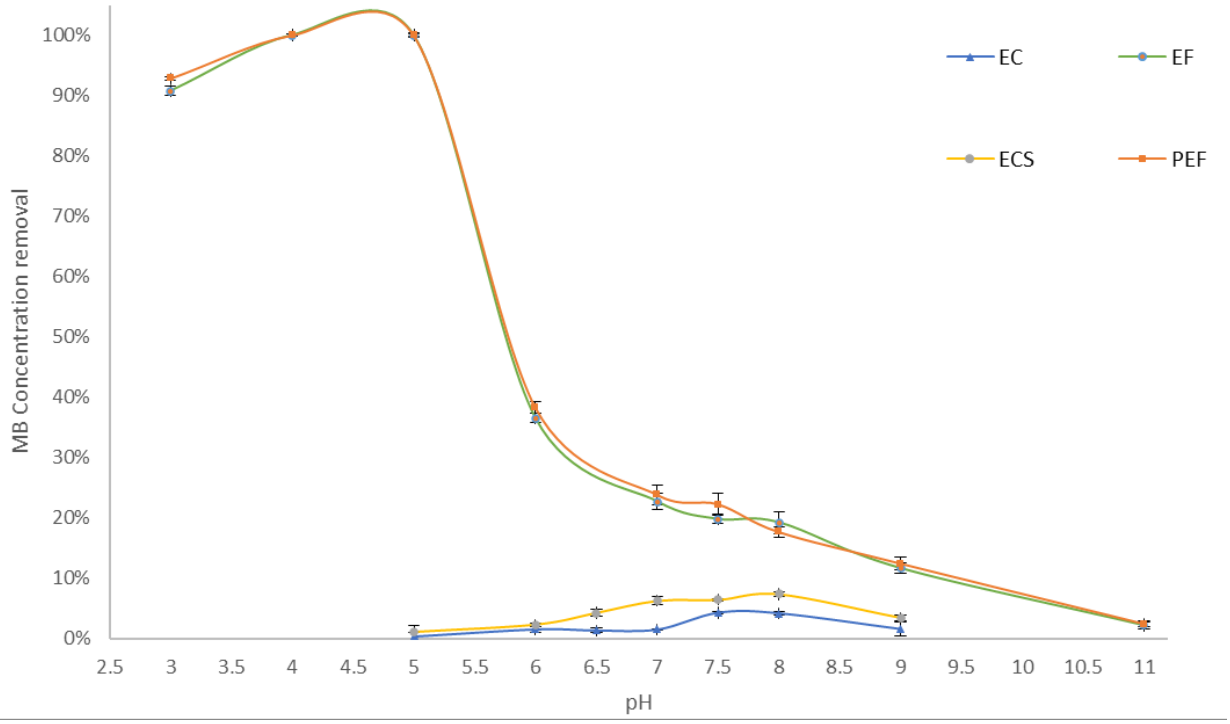

Figure 5.a: MB concentration removal vs pH for EC, ECS, EF and PEF

*Only the points are the real observations. The joining lines between two points in the figure are merely for the purpose of guiding the eye.

The MB removal in EF and PEF show a reducing trend with increasing pH. In EC and ECS there is an increase from pH 6 to pH 8 before decrease.

The concentration values are available in Table 1.a and Table 1.b in Appendix.

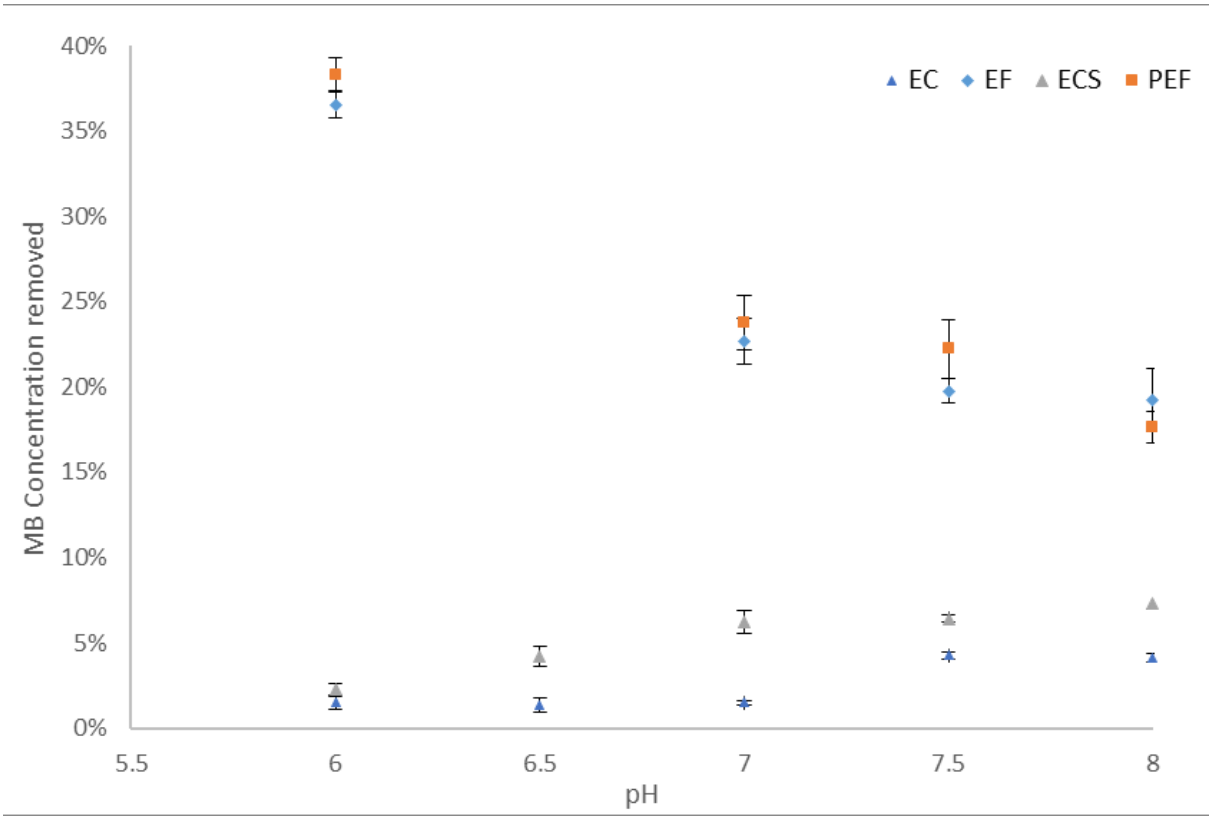

Figure 5.b: This is a zoomed in version of Figure 5.a and represents the drinking water pH range

It shows MB concentration reduction vs pH in the drinking water range of pH 6.5-8. EF and PEF both show high removal capacity in comparison to EC and ECS. ECS is performing better than EC.

4.2 Statistical Analysis

One-way ANOVA was performed on the final concentration readings (post-experiment) obtained across the pH 5 - 9 for EC, ECS, PEF and EF.

Ho: μ EC = μ ECS = μ EF = μ PEF

Ha: Means are not equal

$\alpha = 0.05$

p-value = 0.030, F-value = 3.63, F-critical = 3.09

F-value > F-critical and $p < 0.05$

Therefore, the null hypothesis is rejected and there is significant difference in the mean values.

Check Table 3.c in the Appendix for complete table.

t-tests were performed between the final concentration values of EC and ECS and, between EF and PEF.

For EC and ECS:

Ho: μ EC = μ ECS

Ha: μ EC ≠ μ ECS

α = 0.05

t-stat = 4.08, t-critical = 2.44, p-value = 0.006

t-stat > t-critical and p < 0.05

Therefore, the null hypothesis is rejected and there is a significant difference between the means of EC and ECS.

Check Table 3.a in the Appendix for complete table.

For EF and PEF:

Ho: μ EF = μ PEF

Ha: μ EF ≠ μ PEF

α = 0.05

t-stat = 0.294, t-critical = 2.44, p-value = 0.778

t-stat < t-critical and p > 0.05

Therefore, the null hypothesis is accepted and there is no significant difference between the means of EF and PEF.

Check Table 3.b in Appendix for complete table.

4.3 MB concentration removed vs CD

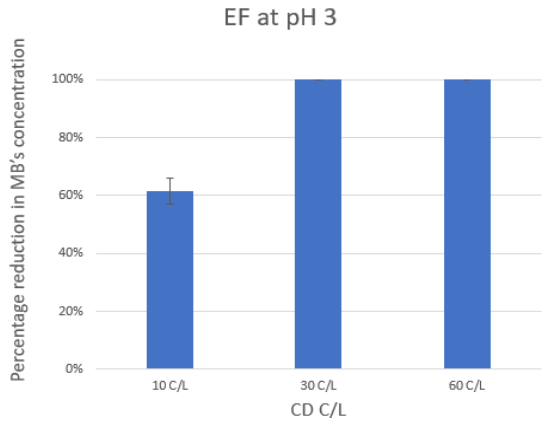

Figure 6.a

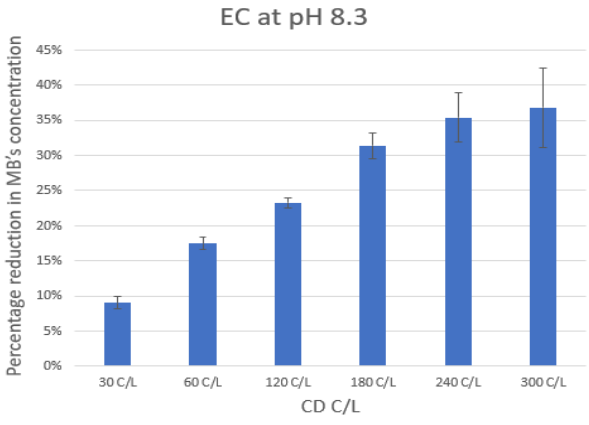

Figure 6.b

Tests for MB concentration reduction for EC and EF at varying CDs

In EF, the MB concentration removal reaches 100% at a low pH (3) of 30 C/L while in EC, the concentration removal rises steadily upto 300 C/L at pH (8.3) but the removal rate is decreasing. The concentration values are available in Table 4.a and Table 4.b in the Appendix.

4.4 Control Volume

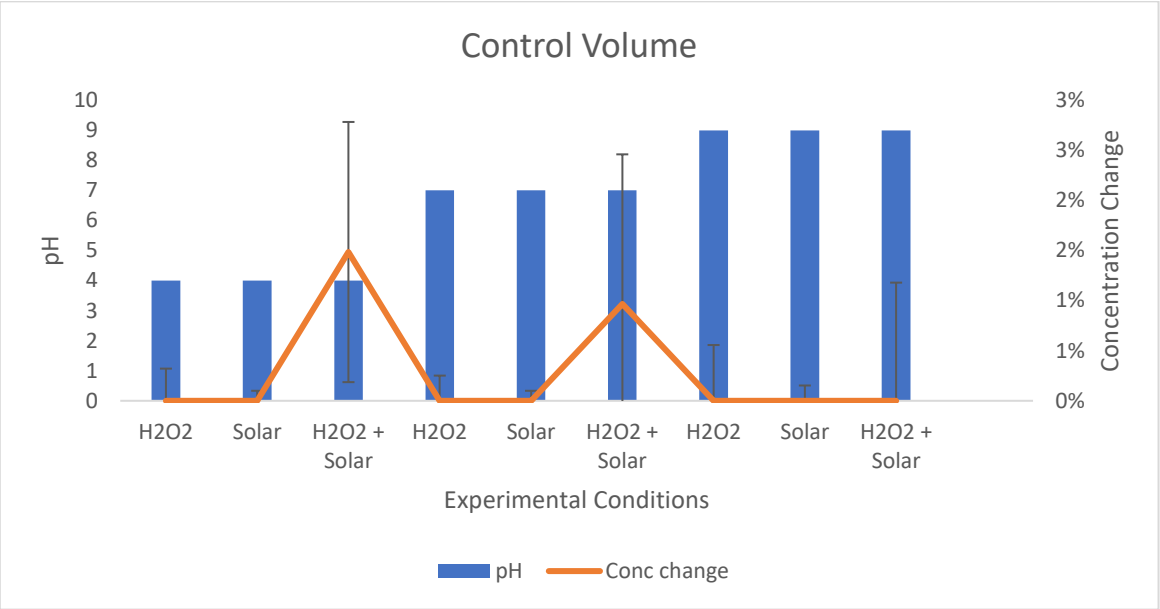

Figure 7: Control volume experiments

H2O2 and Solar, have no concentration reduction of MB at pH 4, 7 and 9 while H2O2 and Solar shows slight reduction in concentration at pH 4 (1.49%) and pH 7 (0.97%) albeit high standard deviation. The concentration values are available in Table 2 in the Appendix.

5. Discussions

1. **Dependence of MB removal on the electrocoagulation type- EC, ECS, EF and PEF**

It has been observed that the MB removal in case of EF and PEF is much higher in comparison to normal EC as well as in PE. This is primarily due to the excess ·OH production because of H_2O_2 in photo-fenton reactions. The combination of ·OH radicals and the photolytic action of irradiation creates a synergistic effect (**Brillas, 2020**)- which is seen in case of EC and ECS. The t-test for EC and ECS also showed that there is a significant difference between their mean values, which could be explained by the radiation effect. On using t-test on the change in the concentration between EF and PEF (section 4.2), it was found that $p > 0.05$. This indicates that there's no significant concentration change when electro-fenton process is done in the presence of sunlight. Visual inspection of curved 5.a also shows that EF and PEF follow a very same pattern. The result is not in accordance with a previous study by **Khataee et. al., 2010**, in which additional production of ·OH from H_2O_2 and hence photolysis of organics had occurred. However, in the above study, UV-C light was employed while in another study $\lambda >$ 300 nm has also shown to have increased ·OH formation (**Barillas, 2020**). The non-deployment of UV-C/ lack of flexibility in changing the wavelength of radiation could be the reason for the lack of differentiation of EF and PEF across the pH range. Natural solar radiation could be affected by factors such as daylight hours and climatology, which may affect the OMP removal. A combination of EC in artificial UV-C irradiation followed by solar irradiation could be an effective treatment method (**Brillas, 2020**).

2. Effect of initial pH

In case of both PEF and EF, it was observed that MB removal is high at low pH (Figure 5.a) and decreases rapidly as the pH increases. The decrease can be attributed to the nature of reactive species produced and the non-radical decay of H_2O_2. The nature of reactive species produced varies with pH such that ·OH radicals are produced at low pH and Fe(IV) radicals at neutral pH (**Ioannis A. Katsoyiannis et. al., 2008**) (**Yufan et. al., 2022**). It has also been observed that ·OH is a more reactive species than Fe(IV) (**Hug S. J. et. al. 2003**) (**Yufan et. al., 2022**). This also explains the fluctuations in the rate of decrease in concentration change with pH since a change in the intermediate reacting species will have an impact on the concentration removal capability of the system. At higher pH non-radical decay of H_2O_2 occurs, which is, the breakdown of H_2O_2 to H2O/OH- directly without the intermediate step of ·OH production (**Pham, A. L. T., et. al, 2009**).

On inspecting the concentration removal in case of EC and ECS, it is observed that MB removal increases from pH 5 to pH 8 (Figure 5.a and 5.b). At neutral and higher pH, the Fe(III) flocs are formed and can promote adsorption (**Mohamed S. Mahmoud, 2013**) (**Fatiha Zidane, et. al. 2008**). At higher pH, sweep flocculation also has an impact as the contaminant (MB) gets enmeshed in the growing floc and is removed (**Jinming et. al., 2003**). This can counteract the generation of weaker intermediate species at high pH.

The figure 5.a and 5.b also reflects higher removal in case of PEF and EF compared to EC and ECS at high pH despite the onset of weaker Fe(IV) species. The result is similar to previous studies in which H_2O_2 addition has a positive impact on the removal, notwithstanding the pH (**Gong et. al., 2017**).

The resulting curve in figure 5.a also proves the hypothesised curve in figure 2 to be incorrect.

3. MB removal mechanism

The scope of research does not cover what proportions of MB removal at a given pH can be attributed to anodic oxidation or radicals or adsorption of MB onto Fe (III) flocs. A previous study on the removal of OMPs- estrogenic compounds through iron electrocoagulation highlighted that 55-68% of removal was due to anodic oxidation, <= 22% with ROS and up to 22% for adsorption (**Maher et. al., 2019**). Given the wide range in the concentration removal through various mechanisms, it can be deduced that each OMP will need to be studied separately to understand their concentration removal mechanisms and results for one OMP cannot be extrapolated accurately to another OMP. However, for the tasks involving engineering optimization, experimenting with a cocktail of OMPs or samples from natural condition should be considered a better approach in order to find the best removal conditions.

4. Radiation wavelength

The solar simulator for the experiments worked at an irradiance of 65 W/m2 and wavelength 300-400 nm. It must be noted that the generation of hydroxyl radicals varies with the type of UV (A, B, C) and is more effective under UV-C ranging from 100-280 nm (**S. Gligorovski et al., 2015**).

The reaction is given by:

$$H_2O_2 + h\nu\ (\text{UV-C}) \longrightarrow 2\ {}^{\cdot}OH \qquad (12)$$

Hence, lesser hydroxyl radicals were generated in the current study due to radiation exposure of 300-400 nm. However, most of the desired radiation does not reach the earth's surface due to the absorption of radiation below 300 nm by ozone and oxygen in the atmosphere (**William H. Brune, 2022**). A solar simulator approximately imitates the radiation from the sun and in this experiment, provides information on MB removal by EC in presence of the sun. However, if the objective of the study is to deduce peak removal under radiation, a lamp with a more specific wavelength range, ideally UV-C range, needs to be used.

5. Control volume experiment

The control experiment (figure 7) in which the water containing MB was dosed with hydrogen peroxide and put in a solar simulator for 6 minutes shows slight peaks in the concentration removal of MB at pH 4 (1.49% removal) and at pH 7 (0.97% removal). This is in accordance to previous studies which indicate that H_2O_2 undergoes photolysis in the presence of primarily UV light (wavelength 100-400 nm) and leads to the production of ·OH radicals (**S. Gligorovski et al., 2015**). The ·OH produced can in turn degrade the dye. However, there's an issue of potential scavenging of ·OH by H2O2 itself and hence, limited radicals are available for dye degradation, explaining why the removal is limited from 0.97% to 1.49%.

6. Effect of charge dosage

In figure 6.a and 6.b effects of charge dosage on the MB removal were studied for EC and EF. In both the cases, increasing charge dosage increases the MB removal. As per Faraday's Law (equation 9), dosage of iron increases with increases in the charge dosage. This will result in increased ROS generation as well as more Fe (III) flocs for adsorption (**Farhadi S. et. al., 2012**).

7. Anode passivation

With regular usage of the apparatus, the anode surface starts showing signs of rust and develops pits. This surface rusting known as anodic passivation reduces the iron dissolution efficiency (Faraday efficiency) at the anodes (**Lakshmanan et. al., 2009**). This issue was resolved by cleaning the anode with a sandpaper after every 4 experiments, which fits well with the earlier studies that consider mechanical cleaning as the most efficient and effective method for removing anode passivation (**Xin Lin et. al., 2023**). Another method which was deployed was exchanging anode and cathode every 2 experiments.

8. Errors in the experiment

The error bars in the experiment were on the higher side, which was due to high standard deviations which can be mainly attributed to the random errors. Since the analytical weighing scale and photo spectrometer have low errors and hence the systematic errors are lower. The multiple steps which required manual accuracy in terms of the mass measurements and pH maintenance would have contributed to the random errors. However, the old pipettes do tend to have larger errors and since the experiment involved multiple steps of pipetting, the systematic errors would have increased. The experiments for the effect of charge dosage on MB removal were performed in triplicates while owing to paucity of time, the experiments studying the effect of pH on MB removal were performed in duplicates. Also, it needs to be noted that during solar simulation, the chamber is completely closed and hence the pH cannot be controlled. Therefore, during the run-time of 6 minutes in the solar simulator, the pH was not controlled strictly.

6. Conclusion

Post study, the following conclusions were drawn:

- Exposure to solar radiation had a significant impact on MB removal in the case of EC and ECS.
- Impact of solar radiation was inconclusive in case of PEF when compared to EF.
- The average MB removal among the four different experiments is PEF/EF > ECS > EC.
- The impact of solar radiation could be less or more pronounced depending upon the wavelength of the radiation.
- At low pH, MB removal is mainly done by the ROS (.OH) while at neutral and higher pH, the weaker ROS (Fe(IV)) is produced and therefore adsorption of MB by Fe(III) flocs has an important contribution.

7. Recommendations

- There is a need for further studies for better differentiation between the contributions in MB removal by ROS and by adsorption. It can be done by developing adsorption isotherms at specific pH values.
- Solar simulator has a limitation that it provides radiation only in the range of 300-400 nm while many studies conducted in other wavelengths have shown better results in ROS production. Therefore, studies with lamps producing specific wavelengths such as UV-C lamp could be a better option for studying the impact of ROS generation.
- Owing to the vast fluctuations in the removal mechanism of different OMPs in water during electrocoagulation, for engineering optimization, it is better to perform the similar tests on a cocktail of OMP's or water from site.
- The ECS process can also be utilised as a method of disinfection post further studies.
- Owing to low contact time (6 minutes), in most of the experiments the MB was not removed completely. In order to understand the energy efficiency of the system, complete MB removal at drinking water pH could be performed to study the economic feasibility of such OMP removal methods.

Acknowledgements

I would like to thank Prof. Dr. Ir. Doris van Halem for her guidance throughout the study which helped in shaping the objectives and the processes in the study. I would also like to thank Ir. Mrinal Roy whose mentorship through hands-on approach, theoretical discussions and numerous lab sessions helped not only with the research but also in developing my interest in electrochemistry. Special thanks to Armand Middeldorp, Lab Technician, WaterLab, whose resourcefulness was a key contributor towards smooth day-to-day working in the lab.

This report is a part of the fulfilment of the course Additional Graduation Work (CIE 5050-09).

8. References

- Amparo Fernández-Pérez, Teresa Valdés-Solís, Gregorio Marbán. 2019. Visible light spectroscopic analysis of Methylene Blue in water; the resonance virtual equilibrium hypothesis. Dyes and Pigments, Volume 161, 2019, Pages 448-456, ISSN 0143-7208, https://doi.org/10.1016/j.dyepig.2018.09.083.
- Bandaru SRS, van Genuchten CM, Kumar A, Glade S, Hernandez D, Nahata M, Gadgil A. 2020. Rapid and Efficient Arsenic Removal by Iron Electrocoagulation Enabled with in Situ Generation of Hydrogen Peroxide. Environ Sci Technol. 2020 May 19;54(10):6094-6103. doi: 10.1021/acs.est.0c00012. Epub 2020 Apr 30. PMID: 32315523.
- Brillas E. 2020. A review on the photoelectro-Fenton process as efficient electrochemical advanced oxidation for wastewater remediation. Treatment with UV light, sunlight, and coupling with conventional and other photo-assisted advanced technologies. Chemosphere. 2020 Jul;250:126198. doi: 10.1016/j.chemosphere.2020.126198. Epub 2020 Feb 17. PMID: 32105855.
- Brillas, Enric. 2020. A review on the photoelectro-Fenton process as efficient electrochemical advanced oxidation for wastewater remediation. Treatment with UV light, sunlight, and coupling with conventional and other photo-assisted advanced technologies, Chemosphere, Volume 250, 2020, 126198, ISSN 0045-6535.
- Bruno Bicudo, Doris van Halem, Shreya Ajith Trikannad, Giuliana Ferrero, Gertjan Medema. 2020. Low voltage iron electrocoagulation as a tertiary treatment of municipal wastewater: removal of enteric pathogen indicators and antibiotic-resistant bacteria, Water Research, Volume 188, 2021, 116500, ISSN 0043-1354, https://doi.org/10.1016/j.watres.2020.116500.
- CCNMLT - Columbia Centre for New Media Learning and Teaching. QMSS e-Lessons. Accessed: 5th October, 2022. (https://ccnmtl.columbia.edu/projects/qmss/).
- D. Ghernaout, M. Aichouni, M. Touahmia. 2019. Mechanistic insight into disinfection by electrocoagulation—A review Desalination and Water Treatment, Desalination Publications (2019). https://doi.org/10.5004/dwt.2019.23457.
- Deng, Y., & Zhao, R. (2015). Advanced Oxidation Processes (AOPs) in Wastewater Treatment. Curr Pollution Rep 1, 167–176.
- Djamel Ghernaout. 2013. Advanced oxidation phenomena in electrocoagulation process: a myth or a reality?, Desalination and Water Treatment, 51:40-42, 7536-7554, DOI: 10.1080/19443994.2013.792520.
- European Commission. 2020. COMMISSION IMPLEMENTING DECISION (EU) 2020/1161 of 4 August 2020. establishing a watch list of substances for Union-wide monitoring in the field of water policy pursuant to Directive 2008/105/EC of the European Parliament and of the Council. Brussels: Official Journal of the European Union.
- F.W. Gaspar, R. Castorina, R.L. Maddalena, M.G. Nishioka, T.E. Mckone, A. Bradman. 2014. Phthalate exposure and risk assessment in California child care facilities. Environ. Sci. Technol., 48 (2014), pp. 7593-7601.
- Farhadi S, Aminzadeh B, Torabian A, Khatibikamal V, Alizadeh Fard M. . 2012. Comparison of COD removal from pharmaceutical wastewater by electrocoagulation, photoelectrocoagulation, peroxi-electrocoagulation and peroxi-photoelectrocoagulation processes. J Hazard Mater. 2012 Jun 15;219-220:35-42. doi: 10.1016/j.jhazmat.2012.03.013. Epub 2012 Mar 14. PMID: 22464981.
- Fatiha Zidane, Patrick Drogui, Brahim Lekhlif, Jalila Bensaid, Jean-François Blais, Said Belcadi, Kacem El kacemi. 2008. Decolourization of dye-containing effluent using mineral coagulants produced by electrocoagulation, Journal of Hazardous Materials,

Volume 155, Issues 1–2, 2008, Pages 153-163, ISSN 0304-3894, https://doi.org/10.1016/j.jhazmat.2007.11.041.
- Genuchten, Case & Peña, Jasquelin & Amrose, Susan & Gadgil, Ashok. (2014). Structure of Fe(III) precipitates generated by the electrolytic dissolution of Fe(0) in the presence of groundwater ions. Geochimica et Cosmochimica Acta. 127. 285–304. 10.1016/j.gca.2013.11.044.
- Gong, Chenhao & Zhang, Zhongguo & Zhang, Jian & Li, Shan. 2017. The addition of hydrogen peroxide in the electrocoagulation treatment for improving toxic organic matters removal: A comparative study. Separation Science and Technology. 52. 10.1080/01496395.2017.1281956.
- Gregory J. 2005. Coagulation and flocculation. CRC Press. London; 2005. doi:https://doi-org.tudelft.idm.oclc.org/10.1680/bwtse.63341.
- Hug, S. J.; Leupin, O. Iron-catalyzed oxidation of arsenic(III) by oxygen and by hydrogen peroxide: pH-dependent formation of oxidants in the Fenton reaction Environ. Sci. Technol. 2003 37 2734 2742.
- Ioannis A. Katsoyiannis, Thomas Ruettimann, and Stephan J. Hug. 2008. pH Dependence of Fenton Reagent Generation and As(III) Oxidation and Removal by Corrosion of Zero Valent Iron in Aerated Water Environmental Science & Technology 2008 42 (19), 7424-7430 DOI: 10.1021/es800649p.
- Jafarzadeh NA. Daneshvar N. Treatment of Textile Wastewater Containing Basic dyes by EC Process. J Water Wastewater. 2006; 57: 22-29.
- Jinming Duan, John Gregory, Coagulation by hydrolysing metal salts, Advances in Colloid and Interface Science, Volumes 100–102, 2003, Pages 475-502, ISSN 0001-8686, https://doi.org/10.1016/S0001-8686(02)00067-2.
- Khataee AR, Fathinia M, Aber S, Zarei M. 2010 Optimization of photocatalytic treatment of dye solution on supported TiO2 nanoparticles by central composite design: intermediates identification. J Hazard Mater. 2010 Sep 15;181(1-3):886-97. doi: 10.1016/j.jhazmat.2010.05.096. Epub 2010 Jun 8. PMID: 20566244.
- Lakshmanan, D.; Clifford, D. A.; Samanta, G. 2009. Ferrous and ferric ion generation during iron electrocoagulation. Environ. Sci. Technol. 2009, 43, 3853– 3859, DOI: 10.1021/es8036669.
- Li, L., Genuchten, C. M., Addy, S. E., Yao, J., Gao, N., & Gadgil, A. J. 2012. Modeling As(III) Oxidation and Removal with Iron Electrocoagulation in Groundwater. Environmental Science & Technology , 46 (21), 12038–12045.
- Longqian Xu, Guangzhu Cao, Xiaojun Xu, Shuli Liu, Zhengyang Duan, Changhua He, Yao Wang, Qihua Huang. 2017. Simultaneous removal of cadmium, zinc and manganese using electrocoagulation: Influence of operating parameters and electrolyte nature, Journal of Environmental Management, Volume 204, Part 1, 2017, Pages 394-403, ISSN 0301-4797, https://doi.org/10.1016/j.jenvman.2017.09.020.
- M. Kobya, E. Demirbas, F. Ulu. 2016. Evaluation of operating parameters with respect to charge loading on the removal efficiency of arsenic from potable water by electrocoagulation. Journal of Environmental Chemical Engineering, Volume 4, Issue 2, 2016, Pages 1484-1494, ISSN 2213-3437, https://doi.org/10.1016/j.jece.2016.02.016.
- Maher, E., O'Malley, K., Heffron, J., Huo, J., Wang, Y., Mayer, B., & McNamara, P. (2019). Removal of estrogenic compounds: Via iron electrocoagulation: Impact of water quality and assessment of removal mechanisms. . Environmental Science Water Research & Technology, The Royal Society of Chemistry.
- Mohamed S. Mahmoud, Joseph Y. Farah, Taha E. Farrag. 2013. Enhanced removal of Methylene Blue by electrocoagulation using iron electrodes, Egyptian Journal of Petroleum, Volume 22, Issue 1, 2013, Pages 211-216, ISSN 1110-0621, https://doi.org/10.1016/j.ejpe.2012.09.013.

- P. Asaithambi, Abdul Raman Abdul Aziz, Wan Mohd Ashri Bin Wan Daud. 2016. Integrated ozone—electrocoagulation process for the removal of pollutant from industrial effluent: Optimization through response surface methodology, Chemical Engineering and Processing: Process Intensification, Volume 105, 2016, Pages 92-102, ISSN 0255-2701, https://doi.org/10.1016/j.cep.2016.03.013.
- Pham, A. L. T.; Lee, C.; Doyle, F. M.; Sedlak, D. L. A. 2009. Silica- 849 Supported Iron Oxide Catalyst Capable of Activating Hydrogen 850 Peroxide at Neutral pH Values. Environ. Sci. Technol. 2009, 43, 8930− 851 8935.
- Rosal R, Rodríguez A, Perdigón-Melón JA, Petre A, García-Calvo E, Gómez MJ, et al. 2010. Occurrence of emerging pollutants in urban wastewater and their removal through biological treatment followed by ozonation. Water Resources;44:578–88.
- S. Gligorovski, R. Strekowski, S. Barbati, D. Vione. 2015. Environmental implication of hydroxyl radicals (OH). Chem. Rev., 115, pp. 13051-13092.
- Shiwei Xie, Chang Li, Peng Liao, Jingfu Wang, Jingan Chen, Ao Qian, Yan Zhang, Taoyuan Wei, Dong Cheng, Mengqi Jia (2022). Experimental and modeling evidence of hydroxyl radical production in iron electrocoagulation as a new mechanism for contaminant transformation in bicarbonate electrolyte. Water Research, Volume 220, 2022, 118662, ISSN 0043-1354.
- Southworth, B. A., & Voelker, B. M. (2003). Hydroxyl Radical Production via the Photo-Fenton Reaction in the Presence of Fulvic Acid. Environmental Science & Technology, 37 (6), 1130-1136.
- Susan Amrose, Ashok Gadgil, Venkat Srinivasan, Kristin Kowolik, Marc Muller, Jessica Huang & Robert Kostecki (2013) Arsenic removal from groundwater using iron electrocoagulation: Effect of charge dosage rate, Journal of Environmental Science and Health, Part A, 48:9, 1019-1030, DOI: 10.1080/10934529.2013.773215.
- Wegelin, Martin & Gechter, Daniel & Hug, Stephan & Mahmud, Abdullah & Motaleb, Abdul. 2000. SORAS - a simple arsenic removal process.
- Weiss, SF, Christensen, ML, Jørgensen, MK. Mechanisms behind pH changes during electrocoagulation. AIChE J. 2021; 67(11):e17384. https://doi-org.tudelft.idm.oclc.org/10.1002/aic.17384.
- William H. Brune. METEO 300 Fundamentals of Atmospheric Science (2022). PennState College of Earth and Mineral Sciences. John A Dutton e-Education Institute. Chapter 6 (Atmospheric Radiation). Accessed (29th September, 2022).
- Xin Lin, Junda Gong, Hang Li, Haiyun Zhang, Yang Yu, Wenyi Tan. 2023. Solar-powered electrocoagulation treatment of wet flue gas desulfurization wastewater using dimensionally stable anode and induced electrode. Environmental Engineering Research **2023,** *28* (1) , 210596-0. https://doi.org/10.4491/eer.2021.596.
- Yufan Chen, Christopher J. Miller, and T. David Waite. 2022. pH Dependence of Hydroxyl Radical, Ferryl, and/or Ferric Peroxo Species Generation in the Heterogeneous Fenton Process. Environmental Science & Technology 2022 56 (2), 1278-1288 DOI: 10.1021/acs.est.1c05722.

Appendix

Readings

pH	Final Average MB Concentration (mg/L)		Concentration Removed		SD	
	EC	ECS	EC	ECS	EC	ECS
5	2.17	1.99	0.330%	0.990%	0.7%	1.2%
6	2.30	2.12	1.49%	2.25%	0.4%	0.4%
6.5	2.21	2.10	1.33%	4.22%	0.4%	0.6%
7	2.18	2.07	1.49%	6.23%	0.14%	0.7%
7.5	2.12	2.04	4.25%	6.41%	0.2%	0.2%
8	2.14	1.98	4.14%	7.34%	0.2%	0.5%
9	2.12	2.13	1.57%	3.37%	1.2%	0.5%

Table 1.a: Experimental data for EC and ECS

pH	Final Average MB Concentration (mg/L)		Concentration Removed		SD	
	EF	PEF	EF	PEF	EF	PEF
3	0.199	0.158	90.7%	92.8%	0.7%	0.3%
4	0	0	100%	100%	0.2%	0.2%
5	0	0	100%	100%	0.4%	0.19%
6	1.36	1.32	36.5%	38.3%	0.8%	1.0%
7	1.72	1.73	22.7%	23.8%	1.4%	1.6%
7.5	1.73	1.73	19.8%	22.2%	0.7%	1.8%
8	1.76	1.83	19.2%	17.6%	1.8%	0.9%
9	1.94	1.89	11.6%	12.4%	0.9%	1.1%
11	2.14	2.13	2.15%	2.4%	0.5%	0.5%

Table 1.b: Experimental data for EF and PEF

	pH	Concentration Removed	Errors
H_2O_2	4	0.00%	0.32%
Solar	4	0.00%	0.10%
H_2O_2 + Solar	4	1.49%	1.30%
H_2O_2	7	0.00%	0.25%
Solar	7	0.00%	0.10%
H_2O_2 + Solar	7	0.97%	1.49%
H_2O_2	9	0.00%	0.56%
Solar	9	0.00%	0.15%
H_2O_2 + Solar	9	0.00%	1.18%

Table 2: Control Volume Experiment at pH 4, 7, 9

t-Test: Paired Two Sample for Means

	EC	*ECS*
Mean	2.159063	2.061681
Variance	0.001063	0.003683
Observations	7	7
Pearson Correlation	0.190958	
Hypothesized Mean Difference	0	
Df	6	
t Stat	4.078793	
P(T<=t) one-tail	0.003255	
t Critical one-tail	1.94318	
P(T<=t) two-tail	0.006511	
t Critical two-tail	2.446912	

Table 3.a: t-Test for final concentrations in EC and ECS

	EF	*PEF*
Mean	1.206485	1.198691
Variance	0.777305	0.785806
Observations	9	9
Pearson Correlation	0.999252	
Hypothesized Mean Difference	0	
Df	8	
t Stat	0.677388	
P(T<=t) one-tail	0.258633	
t Critical one-tail	1.859548	
P(T<=t) two-tail	0.517266	
t Critical two-tail	2.306004	

Table 3.b: t-Test for final concentrations in EF and PEF

Anova: Single Factor

SUMMARY

Groups	*Count*	*Sum*	*Average*	*Variance*
EC	6	12.91135	2.151891	0.000844
ECS	6	12.33283	2.055472	0.004095
EF	6	8.518168	1.419695	0.520407
PEF	6	8.494235	1.415706	0.521021

ANOVA

Source of Variation	*SS*	*df*	*MS*	*F*	*P-value*	*F crit*
Between Groups	2.85136	3	0.950453	3.633344	0.030571	3.098391
Within Groups	5.231837	20	0.261592			
Total	8.083197	23				

Table 3.c: One way ANOVA for final concentrations in EC, ECS, EF and PEF

CD (C/L)	Final MB Concentration (mg/L)	Concentration Removed	SD
30	1.96	9%	0.3%
60	1.82	17%	0.6%
120	1.66	23%	0.3%
180	1.56	26%	1.7%
240	1.36	37%	1.3%

Table 4.a: MB removal at varying CD with pH 8.3-8.5

CD (C/L)	Final MB Concentration (mg/L)	Concentration Removed	SD
10	0.6	61%	0.3%
30	0	100%	0.6%
60	0	100%	0.3%

Table 4.b: MB removal at varying CD with pH 3

MB calibration

In order to measure the percentage concentration removal, a calibration curve for MB was drawn (Fig) between the MB concentrations and the Absorbance values.

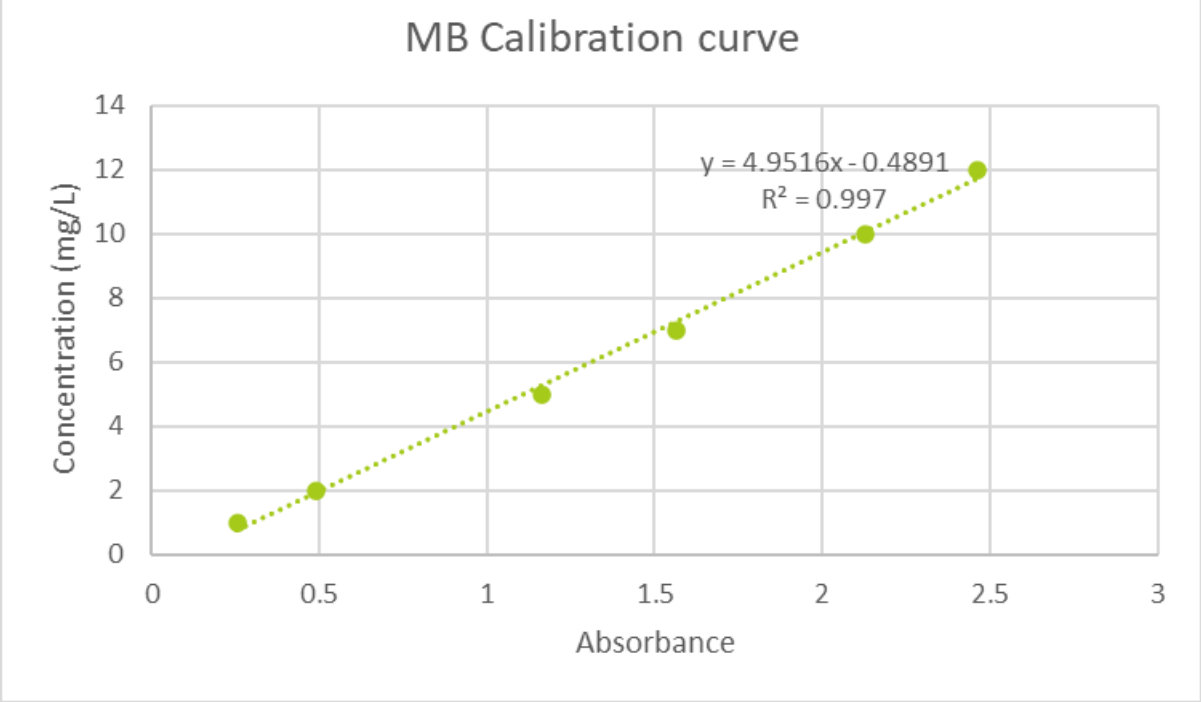

Figure 8: MB Calibration Curve

Energy

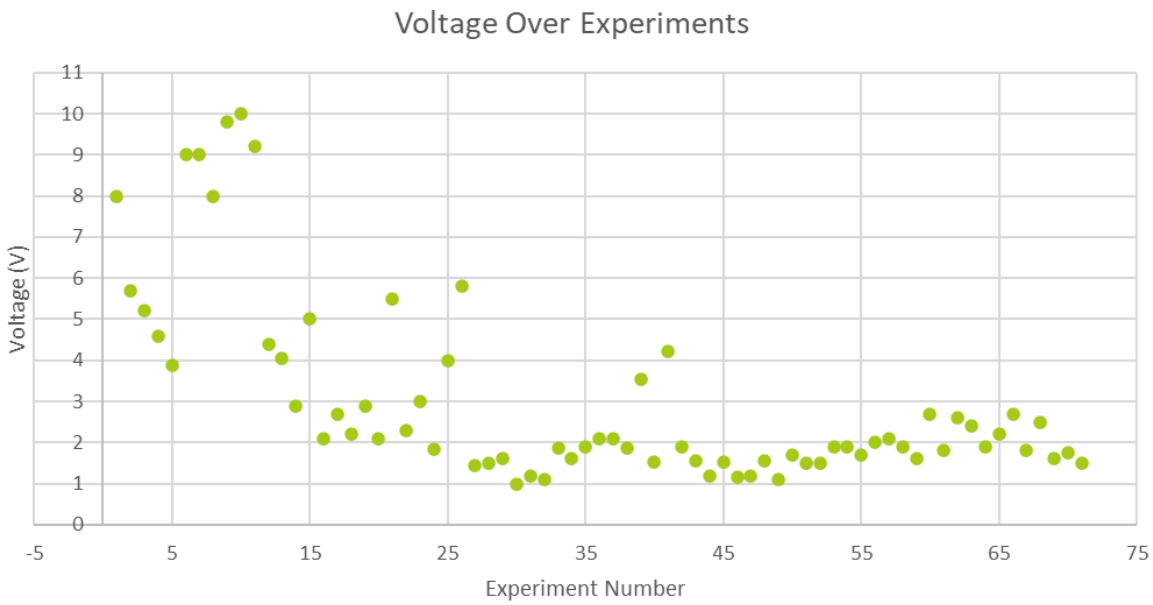

Figure 9: Voltage vs Experiments

Parameter	Mean	Median	Standard Deviation
Voltage (V)	2.2295	1.9	1.058
Energy Consumed (Ws)	0.87	0.74	0.413

Table 5: Energy Consumption per experiment

E = U*I*t*V

where E is the energy consumption (kWh/m3), U is the voltage applied (V), I is the average current (A), t is the reaction times (s) and V is the volume of treated effluent (L).

Cost = Energy consumed + Cost of Iron dissolved (8.68 mg/L)

Safety Plan:

The safety plan for the whole experiment has been set up through the following steps-
The safety plan for the whole experiment has been set up through the following steps-

- Limited number of hours (3 hours * 5 days) for working with Solar lamp
- Use of UV safety goggles during the experimentation
- UV blocking curtains which cover the equipment completely
- The switch off the simulator before opening the lid

- Experimenter will be present at certain distance from the setup at all the times when the experiment is being conducted to ensure safety of the others
- Emergency shutdown card to be placed near the experiment
- After each 6 minute session, the solar simulator is given a rest of 30 minutes to prevent and gas buildup
- Waste (MB) will go be discarded in jerry cans and kept in the waste category 4 (Halogen waste)
- As a by-product of electrocoagulation, extremely minute amount of hydrogen gas (concentration- 0.000311 g/L) is released in the atmosphere. The gas produced can be gotten rid of by simply waiting for few minutes before the next session.
  Calculations are as follows:
  The theoretical concentration of H2 (mg/L), C(H2) is given by Faraday's formula:
  $C(H2)= (Q*M)/(z*F)$
  where Z is the number of electrons involved (equivalents/mol), Q is the charge dosage rate or CDR (Coulombs/L/min), F is Faraday's constant (96,487 C/mol) and M is molecular weight of hydrogen (g/mol).
  Here, Q = 30 C/L/min, Z = 2, M = 2
  C(H2) = 0.000311 g/L, Now water used = 800 mL
  Hence, H2 released = 0.000311g/L * 0.8 L = 0.00025 g